

Identification of Intestinal Pacemaker Frequency through Time-Frequency Ridge Analysis of Surface EEnG

J. Garcia-Casado, *IEEE Member*, Y. Ye-Lin, E. G. Avalos-Gallardo, V. Zena-Gimenez, G. Prats-Boluda, *IEEE Member*

Abstract— The non-invasive monitoring of the frequency of intestinal pacemaker activity (slow wave, SW) has an important diagnostic value. However the presence of noise, physiological interferences and spurious peaks of the spectral estimators can yield to misidentification of SW frequency when using conventional dominant frequency detection method. In this paper, two methods of ridge extraction from the time-frequency distribution of human surface electroenterogram (EEnG) are proposed for the identification and tracking of SW frequency in 13 recording sessions of 120 minutes in 13 healthy volunteers. The minimum average distance method, that includes of information of previous and subsequent windows of analysis, yields the best results in terms of providing ridges that are longer, with less interruptions and with more stable frequency values which better suit the ubiquity and rhythmicity characteristics of the intestinal SW. This technique permits to reduce misinterpretations of intestinal SW frequency which can be of great importance in diagnostic applications of EEnG.

I. INTRODUCTION

Surface EEnG is the small bowel's myoelectrical signal that is recorded on abdominal surface. Intestinal EEnG is made of two components: a pacemaker activity which is called slow wave (SW) and regulates the maximum rhythm of contractions, and the spike bursts (SB) which is associated to the presence and intensity of intestinal mechanical contractions. The analysis of surface EEnG is usually focused on detecting SW frequency [1],[2],[3]. This is mainly because (i) SB activity is hard to be identified and quantified on surface recording due to the insulating and spatial filtering effect of abdominal layers [4], and (ii) it has been proved that pathological situations such as hyperthyroidism and hypothyroidism [5], intestinal ischemia [3] or duodenal distention [6] provoke differences in the frequency values of the SW that go further than inter- and intra-subject variability and hence it has an important diagnostic value.

The intestinal SW is always present in physiological condition and the small intestine exhibits a stepwise gradient in its frequency from about 12 cycles per minute (cpm) in the normal human duodenum to between 9 and 11 cpm in the

jejunum and around 8 cpm in the ileum [7] [3]. At a given point of the small intestine, this frequency is almost constant presenting only slight fluctuations (<1 cpm) with no diurnal variations [5][7]. Moreover, the intersubject variability of the SW frequency is also small (<1.5 cpm in duodenum recordings) [5]. Typically, authors associate the SW frequency to the dominant frequency (DF) of EEnG power spectral density (PSD). Nevertheless, the surface EEnG is severely affected by physiological interference of respiratory and electrocardiographic origin. The typical breathing frequency range for adults at rest (12 - 20 cpm) is very close to the SW frequency (8 - 12 cpm) and lower frequency interference such as baseline drift and gastric myoelectrical activity can also add non-desired components in surface EEnG recordings; and hence additional frequency peaks in the PSD that could be confused with the one associated to SW frequency. Moreover, the PSD estimator can yield spurious frequency peaks that could also provoke misinterpretation of the SW frequency.

In the present paper, two algorithms for SW frequency tracking that consider the ubiquity and rhythmicity characteristics of the intestinal SW are proposed, aiming to reduce the inaccurate identification and misinterpretation of the SW frequency. The signal recording and the proposed algorithms are described in the next section. The results obtained are shown and compared with those of conventional dominant frequency detection method in section III; and the discussion and conclusions are presented in sections IV and V, respectively.

II. MATERIAL AND METHODS

A. Signal recording

Thirteen recording sessions of 120 minutes were carried out in 13 healthy volunteers in fast state (>8h) lying down in supine position inside a Faraday cage. Firstly the abdominal body surface was exfoliated to remove dead skin cells to reduce contact impedance. The abdominal surface was also shaved in male subjects. Three monopolar Ag-AgCl floating electrodes of 8mm of sensing diameter were placed 2.5cm above the umbilicus with an interelectrode distance of 2.5cm. Two bipolar recordings of EEnG were obtained from adjacent monopolar electrodes. In addition, an estimation of Laplacian surface potential was recorded from a tripolar concentric electrode in bipolar configuration (external ring and inner disc are shorted), placed 2.5 cm below the umbilicus. Electrode dimensions and further details can be found in [2]. All signals were amplified and band-pass filtered (0.1-100Hz) by means of commercial bioamplifiers

Research supported in part by the Universidad Politècnica de València (SP20120469; SP20120490) and by Ministerio de Educación y Ciencia (TEC2010-64975).

J. Garcia-Casado, Y. Ye-Lin, V. Zena-Gimenez and G. Prats-Boluda and with Grupo de Bioelectrónica (I3BH), Universitat Politècnica de València, Camino de Vera s/n Ed. 8B Valencia, Spain (phone: +34 963877007 ext. 76027; fax:+34 963877616; e-mails: jgarcia@eln.upv.es, yive@eln.upv.es, vfzena@gbio.i3bh.es, geprabo@eln.upv.es.

E. G. Avalos-Gallardo is with Departamento de Ingeniería electrónica, Instituto tecnológico de Mexicali, Mexico (edgarag87@gmail.com).

(P511, Grass Technologies, Warwick, USA). A disposable electrode placed on the left ankle of the subject was used as reference for the bioelectrical recordings. Signals were simultaneously recorded at a sampling rate of 1kHz.

A 3 axis accelerometer placed on the abdomen was used to detect patient's movements and discard signal segments with artifacts.

B. Frequency tracking and ridges extraction

Most common frequency tracking methods for ridges extraction consist on a two-step process. The first step is obtaining a time-frequency representation of the recorded signals; and the second step consists on applying a chaining algorithm for concatenating local maximum.

In this work, after signal preprocessing (low-pass filtering cut off frequency 2Hz, and down sampling to 4Hz), the time-frequency distribution was obtained by applying an autoregressive spectral estimator of order 120 to moving windows of 120s with steps of 30s (75% overlap). Only the 4 most relevant spectral peaks of each analyzed window were considered for ridge concatenation. Welch modified spectrogram, and different number of significant frequency peaks (3 to 5) were also tested, but provided no better results and therefore are not included in this paper for reasons of space. Also, wavelet transform and scalogram which have been used in other ridge extraction studies [8][9] were discarded since we aim to analyze recording session of 120 minutes and a more computationally effective time-frequency estimator is desired.

Although in physiological conditions the evolution of a ridge associated to the SW activity should be continuous, in practice it could be interrupted due to the presence of noise and other non-desired components. To solve this problem, it is considered that two extracted ridges (r_i and r_j) correspond to the same ridge if their difference in frequency and in time occurrence is smaller than a maximum spectral and temporal lag (λ_f and λ_t , respectively) [8].

$$d_t(E_{ri}, S_{rj}) < \lambda_t \text{ and } d_f(E_{ri}, S_{rj}) < \lambda_f \quad (1)$$

Where E_r and S_r are the final and first nodes of the ridge r ; d_t and d_f are the distance in time and frequency domain.

Considering the ubiquity and rhythmicity characteristics of the intestinal SW [5][7], the parameters λ_f and λ_t were set to 1 cpm and 3 minutes, respectively. Since it is intended to identify the SW frequency and its temporal evolution, only those frequency peaks inside SW normal frequency range (8-12 cpm) were included, and only one frequency value per window can be selected in the chaining process. Regarding the specific algorithm used for chaining the local maxima, two of them were proposed.

– Ridge algorithm 1: Minimum Distance

In this first approach, when multiple successor are available, the ridge of the estimated SW frequency values is formed by concatenating the local maximum of the next temporal window that presents the minimum difference in frequency

(MD) with respect to the actual value of the frequency ridge. This algorithm is similar to the one proposed by [8].

$$MD[k] = \min\{|r[k] - P_j[k+1]| \} \quad (2)$$

Where k is the number of the actual element of the ridge and P_j is the j^{th} significant frequency peak for $j=1 \dots 4$ of the next window of analysis.

If no candidates are found in the $k+1$ window, this process is repeated with the next window as long as the maximum temporal lag (λ_t) is not exceeded.

The first value of the ridge is set to the frequency peak of the first window with minimum distance with the median value of the significant frequency peaks between 8-12cpm of the first three minutes of the session.

– Ridge algorithm 2: Minimum Average Distance

The first method is a simple one, but may provoke ridge interruptions and larger frequency variation since it only considers the information of one adjacent window. To overcome this limitation a new method is proposed. In this case, the information of previous and later windows within temporal lag is taken into account. Precisely, it is computed all the possible trajectories of the ridge from the actual k^{th} element to the $k+5^{\text{th}}$. For every possible trajectory, the average distance (AD) of the trajectory elements respect to the actual reference frequency of the ridge ($r_0[k]$) is calculated. Moreover, in contrast to the first method, the reference frequency of the ridge is not the actual value of the ridge but a weighted average that also considers adjacent previous values of the ridge. Finally, the next element to be concatenated to the ridge is chosen as the one associated to the trajectory of minimum average distance (MAD).

$$AD_n[k] = \sum_{i=1}^{M_n} |r_0[k] - P_j[k+i]| / M_n \quad (3)$$

$$r_0[k] = 0.05 \cdot r[k-4] + 0.1 \cdot r[k-3] + 0.15 \cdot r[k-2] + 0.25 \cdot r[k-1] + 0.45 \cdot r[k] \quad (4)$$

$$MAD[k] = \min\{|AD_n[k]| \} \quad (5)$$

Where $n=1 \dots N$ are the possible trajectories of the ridge from the k^{th} element, M_n is the number of elements of the n^{th} trajectory.

So as to provide greater versatility to the algorithm, the method also permits to skip one window when looking for possible successors and trajectories which modifies equation (3) accordingly.

The first value of the ridge is the same as the first method.

C. Ridges characterization

In order to compare the ridges obtained from the MD and MAD methods, the following characteristic parameters were calculated:

- Ridge length percentage (RL): ratio between the total length of the ridges obtained for a recording session

and the total number of the analyzed windows in that session.

- Number of ridge interruptions (NI) per session
- Average frequency (AF). The mean frequency value of the elements of the ridge
- Average frequency variation (AFV). The mean of the difference between consecutive elements of the ridge.

The last two parameters were also calculated for the traditional method of considering the SW frequency the one associated to the highest frequency peak (dominant frequency, DF) between 8 and 12 cpm, in every analyzed window.

III. RESULTS

Fig. 1 and Fig. 2 show an example on how the two proposed methods for ridges extraction work for a predetermined sequence of significant peak values between 8 and 12 cpm. As shown in Fig. 1, at second 30 the frequency value of the present element of the ridge is 10.2 cpm; and there are two possible successors 9 and 11 cpm. The application of the MD method concatenates the frequency peak of 11cpm at 60s which yields a minimum frequency difference with the present element of the ridge. However, neither the next window (90s) nor the followings within λ_t contain successors with MD minor than λ_f , and hence the ridge is interrupted. Fig. 2 shows the possible trajectories of the ridge after second 30 generated by the MAD method. Trajectories 1 and 2 would concatenate the frequency of 11cpm at 60s to the ridge, whereas trajectories 3 and 4 would chain the 9cpm peak at 60s. Trajectories 5 and 6 are obtained when skipping the adjacent window (60s) and permitting to directly concatenate elements in the next one (90s). The average distance is calculated for every possible trajectory: $AD_1=0.44\text{cpm}$, $AD_2=0.68\text{cpm}$, $AD_3=0.36\text{cpm}$, $AD_4=0.36\text{cpm}$, $AD_5=0.15\text{cpm}$ and $AD_6=0.45\text{cpm}$. In this case, the minimum AD is obtained for trajectory 5, and hence the frequency of 9.8 cpm at 90s would be the element chained to the ridge. As it can be observed trajectory 5 yields a longer ridge and with smoother changes in frequency compared to the one provided by the MD method shown in Fig.1.

Fig. 3 shows the results of applying the proposed frequency tracking and ridge extraction methods to a complete recording session; the application of the traditional method of only considering the dominant frequency between

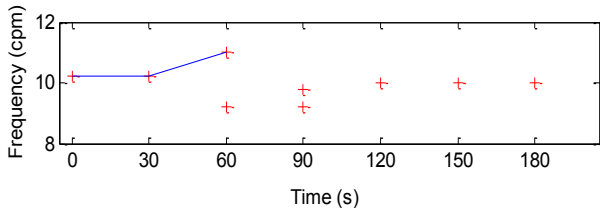


Figure 1. Example of ridge generation with MD method. Red crosses are the local maximum candidates that could be included in the ridge associated to the SW frequency. Blue line connects the elements included in the ridge, which is interrupted at second 60.

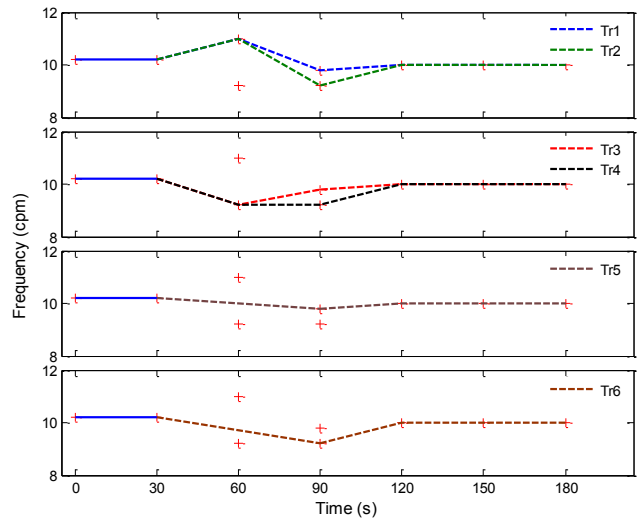


Figure 2. Example of possible trajectories for ridge generation generated with MAD method. Red crosses are the local maximum candidates that could be included in the ridge associated to the SW frequency. Dashed lines connect the elements included in the different possible ridge trajectories. The average distance with the actual reference frequency of the ridge is calculated for every trajectory ($AD_1=0.44\text{cpm}$, $AD_2=0.68\text{cpm}$, $AD_3=0.36\text{cpm}$, $AD_4=0.36\text{cpm}$, $AD_5=0.15\text{cpm}$ and $AD_6=0.45\text{cpm}$).

8 and 12 cpm is also shown (top trace). Red crosses are the local maximum candidates, provided by the time-frequency distribution applied to the experimental data, that could be included in the ridge associated to the SW frequency. It can be clearly observed that the DF method yields large variations in the frequency that cannot correspond to possible physiological changes in the SW frequency. The ridge obtained by MD method reduces such variations. Nonetheless there are segments (e.g. between minutes 65 and 85) in which the trend of the ridge may still not correspond to SW frequency changes. Furthermore, the ridge is interrupted in several occasions (minutes 14, 23, 46, 119) with the MD method. In contrast the ridge obtained with the MAD method is continuous and presents very small fluctuations of the frequency values.

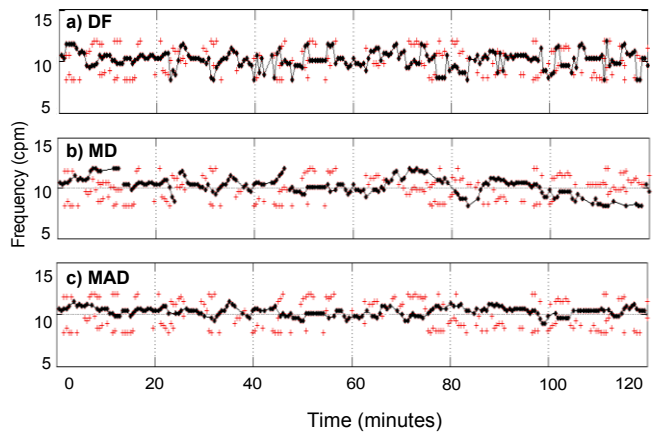


Figure 3. Black line: temporal evolution of the a) dominant frequency between 8-12 cpm; b) ridge obtained with the MD method; c) ridge obtained with MAD method; corresponding to the Laplacian EEnG signal of recording session 6. Red crosses are the local maximum candidates, provided by the time-frequency distribution, that could be included in the ridge associated to the SW frequency.

TABLE I. CHARACTERISTIC PARAMETERS OF THE METHODS TO IDENTIFY SW FREQUENCY (MEAN \pm SD; N=13 RECORDING SESSIONS)

Parameter	Chan.	Method		
		DF	MD	MAD
RL (%)	Lap	--	77.23 \pm 5.56	87.03 \pm 3.99
	Bip1	--	84.86 \pm 5.71	90.24 \pm 5.02
	Bip2	--	83.77 \pm 6.64	88.85 \pm 4.69
NI	Lap	--	2.69 \pm 1.14	1.15 \pm 1.03
	Bip1	--	1.54 \pm 0.75	0.46 \pm 0.63
	Bip2	--	1.77 \pm 1.48	0.77 \pm 0.97
AF (cpm)	Lap	10.23 \pm 1.17	9.98 \pm 0.98	9.86 \pm 0.90
	Bip1	10.56 \pm 1.08	10.41 \pm 0.97	10.33 \pm 0.90
	Bip2	10.06 \pm 0.97	10.28 \pm 0.93	10.32 \pm 0.89
AFV (cpm)	Lap	0.61 \pm 0.11	0.30 \pm 0.05	0.24 \pm 0.02
	Bip1	0.45 \pm 0.09	0.25 \pm 0.04	0.23 \pm 0.01
	Bip2	0.47 \pm 0.09	0.25 \pm 0.04	0.21 \pm 0.02

Table I shows the characteristic parameters used to evaluate the different methods to identify and track SW frequency. Firstly, both ridge concatenation methods proposed (MD and MAD) reduce the variability of the interpreted SW frequencies in comparison with the traditional method of just detecting the DF; which is reflected in the reduction of AFV and in the smaller standard deviation of the AF. Secondly, if we compare MD with MAD, the superior performance of MAD is corroborated since the percentage of analyzed windows which have a frequency value included in a ridge is higher, and the number of ridge interruptions is smaller than those of MD method.

IV. DISCUSSION

The chaining criterion of minimum distance in ridge extraction has proved to provide satisfactory results in the analysis of uterine activity [8]. In this work it also has shown to reduce the non-physiological variability of the estimated SW frequency in comparison to the traditional dominant frequency detection method. Nonetheless, when considering additional information from previous and subsequent windows of analysis, as performed by the MAD method proposed in this paper, the outcome can be even better. This improvement is manifest in terms of providing ridges that are longer, with fewer interruptions and with more stable frequency values which better suit the ubiquity and rhythmicity characteristics of the intestinal SW [5][7].

Notwithstanding, a limitation of this (and most) non-invasive studies of human EEnG is the lack of simultaneous internal signals to be used as a reference to check the estimated SW frequency. Nevertheless, we believe that the frequencies of the extracted ridges are associated to the SW activity for a number of reasons. First, there is no other physiological component in the frequency range of 8-12cpm with the same characteristics. Secondly, the RL is of about 90% suggesting existence along practically the entire session. Additionally, the frequency values of the ridge for every individual recording session are between 9 and 11 cpm with a standard

deviation (not shown) ranging from 0.39 to 0.9 cpm, which are similar to those obtained in other works. Chang et al reported estimated SW frequencies of 10.9 ± 1.0 cpm and of 10.9 ± 1.3 cpm on fasting and postprandial state [1]; and mean SW frequencies between 9.7 and 10.2 were reported in [2]. Finally, although the small bowel is twisted inside the abdominal cavity, the area above the umbilicus could be expected to contain more intestinal loops from the lower duodenum and upper jejunum and therefore yield higher SW frequencies than the area below the umbilicus. Our results are in agreement with this: the frequencies (AF) associated with the intestinal SW from bipolar recordings are higher than those of Laplacian recordings. Lastly, it should be considered that some pathologies such as intestinal ischemia could lead to lower frequency values of SW (<8cpm) [3]. Therefore, the proposed algorithms should be adapted to deal with such circumstances.

V. CONCLUSION

The use of information regarding the physiological characteristics of the SW in frequency tracking and ridge extraction methods permits to reduce inaccurate identification and misinterpretation of the SW frequency. The new proposed method which calculates the minimum average distance using information of previous and subsequent windows of analysis outperforms the simpler method of minimum distance, and the traditional method of dominant frequency detection, what can be of great importance in diagnostic applications of EEnG.

REFERENCES

- [1] F. Y. Chang, C.-L. Lu, C.-Y. Chen, J.-C. Luo, S.-D. Lee, H.-C. Wu, and J. D. Z. Chen, "Fasting and postprandial small intestinal slow waves non-invasively measured in subjects with total gastrectomy," *Gastroenterology*, no. 22, pp. 247-252, 2006.
- [2] J. Garcia-Casado, V. Zena-Gimenez, G. Prats-Boluda, and Y. Ye-Lin, "Enhancement of non-invasive recording of Electroenterogram by means of a flexible array of concentric ring electrodes," *Annals of Biomedical Engineering*, vol. 42, no. 3, pp. 651-660, 2014.
- [3] S. Somarajan, S. Cassilly, C. Obioha, L. A. Bradshaw, and W. O. Richards, "Noninvasive Biomagnetic Detection of Isolated Ischemic Bowel Segments," *IEEE Transactions on Biomedical Engineering*, vol. 60, no. 6, pp. 1677-1684, 2013.
- [4] J. Garcia-Casado, J. L. Martinez-de-Juan, and J. L. Ponce, "Noninvasive measurement and analysis of intestinal myoelectrical activity using surface electrodes," *IEEE Transactions on Biomedical Engineering*, vol. 52, no. 6, pp. 983-991, June 2005.
- [5] J. A. Clifton, J. Christensen, and H. P. Schedl, "The human small intestinal slow wave," *Trans. Am. Clin. Climatol. Assoc.*, vol. 77, pp. 217-225, 1966.
- [6] M. Abo, J. Liang, L. Qian, and J. D. Chen, "Distension-induced myoelectrical dysrhythmia and effect of intestinal pacing in dogs," *Dig. Dis. Sci.*, vol. 45, no. 1, pp. 129-135, Jan. 2000.
- [7] P. Fleckenstein and A. Oigaard, "Electrical spike activity in the human small intestine. A multiple electrode study of fasting diurnal variations," *Am. J. Dig. Dis.*, vol. 23, no. 9, pp. 776-780, Sept. 1978.
- [8] H. Leman and C. Marque, "Ridge extraction from the scalogram of the uterine electromyogram," 1 Ed Pittsburgh, USA: 1998, pp. 245-248.
- [9] P. Tchamitchian and B. Torr sani, "Ridge and Skeleton Extraction from the Wavelet transform," 1990, p. CPT-90-P.2467.